Shankar A., Safronov A., Beketov I.
Chimica Techno Acta. 2017. Vol. 4, No. 3. P. 158–166.
ISSN 2409–5613

DOI: 10.15826/chimtech/2017.4.3.01

Ajay Shankar[1], Alexander Safronov[2,3], Igor Beketov[3]

[1]Indira Gandhi National Tribal University,
Amarkantak, Madhya Pradesh, 484886, India
e-mail: ajayshankar0@gmail.com
[2]Ural Federal University,
19 Mira St., Ekaterinburg, 620002, Russian Federation
e-mail: safronov@iep.uran.ru
[3]Institute of Electrophysics UB RAS,
106 Amundsen St., Ekaterinburg, 620016, Russian Federation
e-mail: beketov@iep.uran.ru

Encapsulation of metallic iron magnetic nanoparticles by polyacrylamide in water suspensions

Theoretical consideration of the factors of the stability of metallic iron magnetic nanoparticles (MNPs) in water suspensions was done using extended DLVO (Derjaguin-Landau-Verwey-Overbeek) approach based on the balance among Van der Waals, electrostatic, magnetic and steric interactions. Magnetic and steric interactions dominate over other in suspensions of Fe MNPs. To test the theory Fe MNPs with average diameter 84 nm were synthesized by electrical explosion of wire and encapsulated by polyacrylamide in water suspension to provide steric repulsion. It was shown that encapsulation resulted in the efficient diminishing of the aggregation of metallic iron MNPs in water.

Keywords: Iron nanoparticles; encapsulation; polyacrylamide.

Received: 28.06.2017; accepted: 24.07.2017; published: 20.10.2017.

Introduction

Magnetic nanoparticles (MNPs) are the subject of intensive research due to the special properties required for technological and biomedical applications such as magnetic fluids, catalysis, magnetic resonance imaging, data storage, and environmental remediation [1–3]. In these applications magnetic material is to be dispersed in a solid phase giving a composite material, or in a liquid giving a ferrofluid or a suspension. Among others iron-based MNPs attract special attention due to their relatively low cost and comparatively low toxicity for the living systems, which is of the major importance for the biotechnological and biomedical applications. In this respect iron oxide MNPs are mostly studied. There are a lot of different methods for their synthesis, a variety of actual and prospective applications [3], and numerous studies of their compatibility [4]. At the same time metallic iron MNPs are less studied. Meanwhile, from the viewpoint of their magnetic properties metallic iron has indisputable advantages over its oxides. Its saturation

magnetization is at least three times higher than that of magnetite. If used in magnetic sensors, actuators, contrast agents for MRS iron MNPs might provide higher sensitivity, better response, and lower detectable doses. However, there are several unresolved problems of the application of metallic iron MNPs in suspensions. The major one is strong aggregation of metallic iron MNPs.

It is known, that the aggregation of nanoparticles is thermodynamically favorable process. The surface between coexisting phases carries on excess free energy, which might be very high for the nanosystem as its specific surface is also high due to small dimensions. The aggregation of MNPs diminishes the surface of the direct contact among the phases and leads to the minimization of the free surface energy [5]. In order to overcome the thermodynamic force for the aggregation and to provide the stability of disperse systems with nanoparticles, such approaches as electrostatic or steric stabilization are used. Unfortunately, the variety of stabilizers, which proved to be successful for the stabilization of iron oxide suspensions, are not such for the suspensions of metallic iron particles in water. It is the result of the enhanced magnetic properties of iron, which dominate over other forces in colloid suspensions.

The objective of the present study was to examine the problem of the stability of magnetic iron nanoparticles from theoretical point of view and experimentally test the possibility of the stabilization of the suspension of spherical iron MNPs in water, using their encapsulation by water-soluble polymer – polyacrylamide.

Experimental

Materials

Metallic iron magnetic nanoparticles (MNP) were synthesized by the method of electric explosion of wire (EEW). The detailed description of EEW equipment designed at the Institute of Electrophysics of RAS (Ekaterinburg, Russia) is given elsewhere [6–8]. The method is based on the evaporation of a portion of metal wire by the electric high power pulse in the explosion chamber filled with the inert atmosphere. Further condensation of the expanding metal vapors resulted in the formation of spherical MNPs. The applied voltage was 30 kV and the length of the exploded portion of wire was 70 mm. The wire was continuously fed to the explosion chamber by the feeding device, the high voltage source was concurrently recharged after each explosion, and the process was repeated in the pulsed manner resulted in rapid production of MNPs (200 g/h). The reaction chamber was filled with a circulating mixture of 70 % of Ar and 30 % of N_2 providing the working gas pressure of 0.12 MPa.

Polyacrylamide (PAAm) was synthesized by the radical polymerization reaction of acrylamide (AAm) (AppliChem, Darmstadt) in 1.6 M water solution at 80 °C. Ammonium persulfate (PSA) in 5 mM concentration was used as an initiator. The reaction mixture was kept at 80 °C for 1 h. The obtained PAAm solution was then diluted with distilled water down to 5 % concentration by weight. The resulted solution was then used as a stock for the encapsulation of iron MNPs. The molar weight of PAAm determined by viscometry was M = 1.46*105 g/mol.

Methods

The powder X-ray diffraction (XRD) patterns were recorded using Bruker D8 Discover with Cu Kα radiation (λ = 1.542 Å) with graphite monochromator. The Rietveld refinement of XRD patterns were performed using Topas-3 software. The morphology of MNPs was examined using JEOL JEM2100 transmission electron microscope (TEM) operating at 200 kV. The specific surface area of MNPs was measured by the low-temperature adsorption of nitrogen (Brunauer-Emett-Teller (BET) approach) using Micromeritics TriStar3000 analyzer. The magnetic measurements were carried out using (Cryogenics Ltd. VSM) vibrating sample magnetometer (VSM) at room temperature for powder samples placed in a gelatine capsule. The magnetization values in a field of 1.8 T were designated as the saturation magnetization values (M_s). Thermal analysis was done using NETZSH STA409 thermal analyzer operated in linear heating mode from 40 to 1000 °C at 10 K/min in the air. Dynamic light scattering (DLS) and electrophoretic light scattering (ELS) measurements were performed using Brookhaven ZetaPlus particle size analyzer: 5 and 3 runs were recorded for hydrodynamic size and zeta-potential measurements, respectively.

Results and their discussion

Theory

The aggregation features of iron MNPs in water suspension can be qualitatively modeled by the extended DLVO approach. In classical DLVO theory, the attractive and repulsive interactions are modeled for van der Waals and electrostatic interactions only. In case of the magnetic colloidal dispersions where both steric and magnetic interactions are also present, they must also be taken into account. The modified approach to consider all these interactions is known as xDLVO approach [9]. This theory was elaborated to study the stability of iron MNPs in water suspension.

The van der Waals interaction energy (V_{vdW}) between MNPs with radius r at a distance s was calculated as [10]:

$$V_{vdW} = \frac{-A(r)}{6}\left[\frac{2r^2}{s(4r+s)} + \frac{2r^2}{(2r+s)^2} + \ln\left\{s\frac{(4r+s)}{(2r+s)^2}\right\}\right], \quad (1)$$

where

$$A(r) = 1.77\times10^{-19} + 1.60\times10^{-19}e^{-r/3.05} + 6.35\times10^{-20}e^{-r/10.75} + 2.05\times10^{-20}e^{-r/52.18}\ [\mathrm{J}].$$

The electrostatic repulsions under constant charge boundary condition were taken as [11]:

$$V_e = 2\pi r\varepsilon_r\varepsilon_o\psi_o^2\ln\left(1+e^{-\kappa s}\right), \quad (2)$$

where

$$\kappa = \left(\frac{k_B T\varepsilon_0\varepsilon_r}{q^2 N_A\sum z_i^2 c_i}\right)^{-1/2}.$$

Here ε_r is the relative dielectric constant of water, ε_0 is the permittivity of free space, ψ_0 is the surface potential, q is the elementary charge, z_i is the charge of simple ions, c_i is their molar concentration, N_A, k_B, and T have their usual meanings. We used the value of electrokinetic (zeta) potential of –16 mV for iron MNPs in water (by ELS) as an approximation for the surface potential.

The steric repulsion was taken into account through a hard core combined with a soft tail potential, as modeled previously under self-consistent field (SCF) theory.

This originating overall steric term for two identical stabilized MNPs was taken as [12]:

$$V_{st} = \begin{cases} \infty & \text{for } s < 0 \\ \left(\frac{r\pi^3\delta^3\sigma_p kT}{12N_p l^2}\right)\left[-\ln\left(\frac{s}{2\delta}\right) - \frac{9}{5}\left(1-\frac{s}{2\delta}\right) + \frac{1}{3}\left(1-\left(\frac{s}{2\delta}\right)^3\right) - \frac{1}{30}\left(1-\left(\frac{s}{2\delta}\right)^6\right)\right] & \text{for } 0 < s < 2\delta \\ 0 & \text{for } s > 2\delta \end{cases} \quad (3)$$

where, δ is thickness of adsorbed LPAAm layer, σ_p is surface density of adsorbed chains, N_p is number of free segments and l is the length of one free segment.

The maximum magnetic attraction energy (V_M) between MNPs was taken as [10]:

$$V_M = \frac{-8\pi\mu_o M^2 r^3}{9\left(\frac{s}{r}+2\right)} \quad (4)$$

The total energy of interaction between iron MNPs was calculated as a combination of equations (1)–(4).

$$V(s) = V_{vdW}(s) + V_e(s) + V_{st}(s) + V_M(s) \quad (5)$$

Considering contributions from different terms in equation (5) it was found out that steric (equation (3)) and magnetic (equation (4)) terms are dominating for iron MNPs. These two terms in turn strongly depend on such parameters of MNPs as the radius, the thickness of the steric protective layer, and the magnetization of particle. Fig. 1 presents the dependence of the energy of interparticle interaction at different combinations of these parameters. The parameters are taken close to that characteristic for the MNPs studied below.

It is noticeable that each curve in Fig. 1 has a minimum, which is the result of the balance among attractive magnetic force and repulsive steric interaction. It is con-

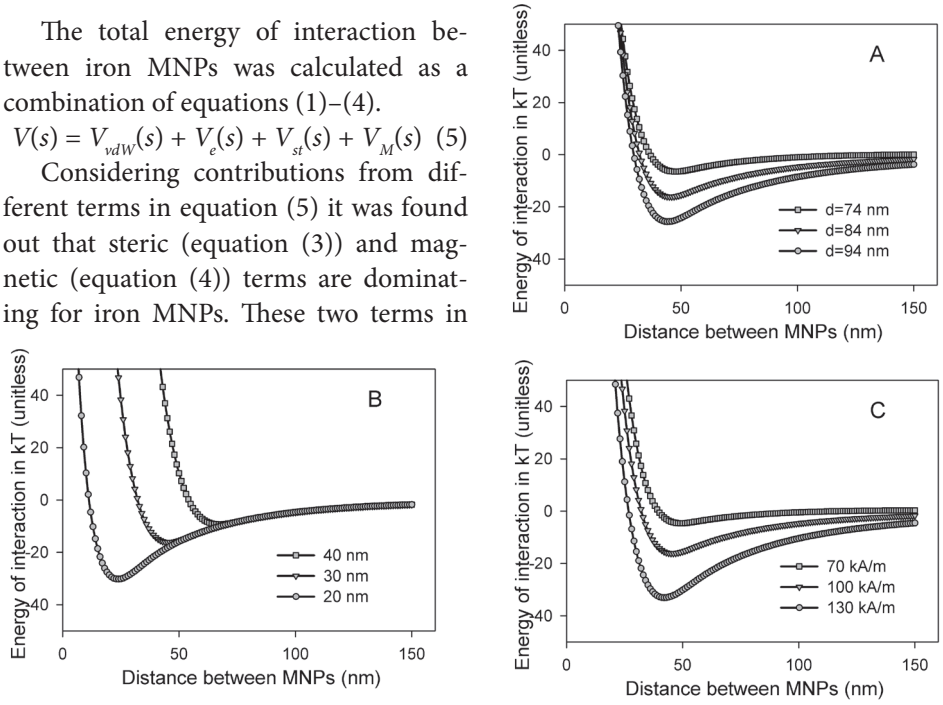

Fig. 1. Energy of interaction as a function of the distance between iron MNPs: A – The influence of the diameter of MNPs at constant thickness of steric layer (30 nm) and constant magnetization (100 kA/m); B – The influence of the thickness of steric layer of MNPs at constant diameter (84 nm) and constant magnetization (100 kA/m); C – The influence of the magnetization of MNPs at constant diameter (84 nm) and constant thickness of steric layer (30 nm)

ventionally accepted that the aggregates can be disrupted by the thermal motion if the corresponding minimum is less than 20 k_BT, as statistically only a few particles will cross barrier in this case [13]. Thus, the depth of the minimum indicates the tendency of the ensemble of MNPs to aggregation. It is obvious that the depth of the minimum increases with the increase of particle radius, with the increase in magnetization, and the diminishing of the thickness of protective layer.

Based on these results, we analyzed the possibility of de-aggregation of Fe MNPs by their encapsulation by polyacrylamide.

Characterization of metallic iron MNPs

Fig. 2 presents TEM image of metallic iron MNPs synthesized by EEW. They are spherical in shape and non-aglomerated. The spherical shape of MNPs is the result of the EEW conditions. The electrical pulse, which passes the portion of wire, provides its overheating to ca 10^4 K and complete vaporization. Then iron MNPs

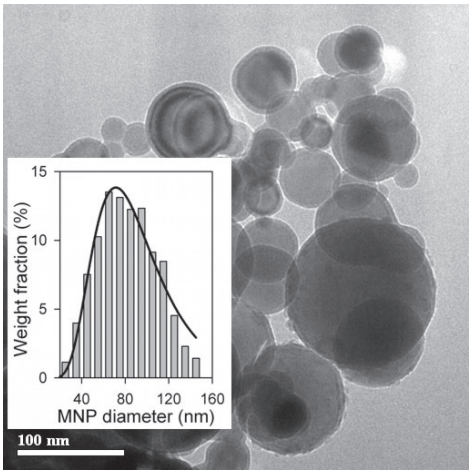

Fig. 2. TEM image of metallic iron magnetic nanoparticles synthesized by electric explosion of wire. Inset: histogram – calculation of particle weight fraction from the image analysis, line – fitting of PSD by equation (6)

are condensed in a vapor phase under the thermodynamic condition for the minimization of free energy. The sphere has a minimal surface among other possible geometrical figures with a constant volume. Hence, the obtained iron MNPs condense in a shape of spheres. The density of vaporized metal in the EEW explosion chamber is kept low by constant circulation of inert working gas; it minimizes the probability of collisions among condensing MNPs and prevents their coalescence in liquid phase. The particle size distribution (PSD) (Fig. 2, Inset), which was obtained by the graphical analysis of more than 2000 images of MNPs, fits well the following lognormal equation:

$$PSD(d) = \frac{10.70}{d} e^{-\frac{(\ln d - \ln(83.9))^2}{2*0.402^2}} \quad (6)$$

The specific surface area of MNPs (Ssp) measured by the low-temperature adsorption of nitrogen was 9.0 m^2/g. The surface average diameter of MNPs, calculated from this value using the equation $d_s = 6/(\rho S_{sp})$ ($\rho = 7.87$ g/cm^3 being iron oxide density) was 84.7 nm. It was in a good agreement with the median diameter 83.9 nm in PSD described by Equation (6) (the latter value was used a basic level in the theoretical calculations given above).

Fig. 3 shows XRD patterns of iron particles. MNPs contain 93 % of α-Fe with a = 2.867(2) Å and coherent length 82(5) nm and 7 % of cubic phase of γ-Fe with a = 3.591(3) Å and coherent length 27(2) nm. The coherent length of α-Fe phase perfectly correlates with the average diameter of Fe MNPs obtained both by the analysis of TEM images and by the calculation based on BET sorption results. It means that each singular MNP is a monocrystalline particle. The coherent length of γ-Fe phase is much lower. Most

likely it means that γ-Fe phase predominantly corresponds to the smallest MNPs in the ensemble.

Magnetic hysteresis loops of iron MNPs (see Fig. 4) are typical for the magnetically soft materials. The low field behavior (inset in Fig. 4) reveals the existence of magnetic hysteresis and coercivity.

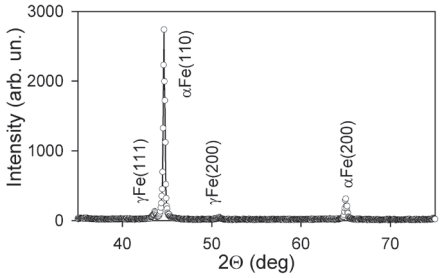

Fig. 3. XRD diffractogram of iron MNPs synthesized by EEW

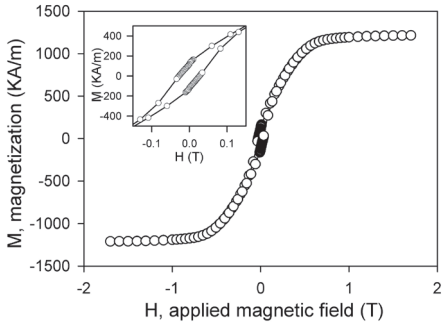

Fig. 4. Magnetic hysteresis loop of Fe MNPs at 25 °C. Inset – enlarged view of hysteresis loop in low fields

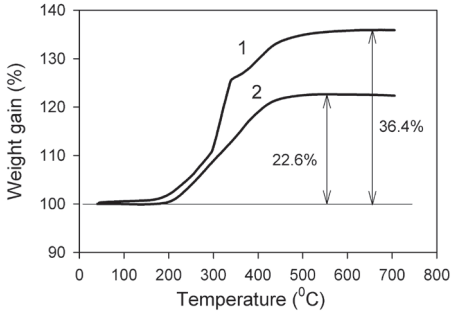

Fig. 5. Thermograms of the heating of pristine MNPs (1) and encapsulated MNPs (2) in the air

It can be understood taking into account that although in the ensemble of spherical iron MNPs with average diameter of about 82 nm the majority of them are in multidomain state, one cannot exclude the presence of a small fraction of single domain MNPs contributing to non-zero coercivity. The value of the saturation magnetization in bulk state for pure iron is M_s = 1710 (kA/m) [14] for room temperature. The obtained value for M_s for MNPs is about 30 % lower. Most likely this difference stems from two reasons. First, there is a thin oxide layer on the surface of iron MNPs, which appear inevitably if the active surface of MNPs is exposed to the air. The layer 5 nm in thickness can not be detected by XRD but as the magnetization of iron oxide is lower, it certainly contributes to the diminishing of M_s values for MNPs. Another possibility is the disturbance of the crystalline structure of iron in several layers adjacent to the surface of a spherical nanoparticle. These layers are not contributing to the ferromagnetic response due to the insufficient number of the nearest neighbours [15]. Both processes are contributing to M_s reduction but it is difficult to make more precise analysis first of all due to the existence of the MNPs size distribution.

Encapsulation of Fe MNPs by PAAm

Encapsulation of iron MNPs was performed by grinding in an agate mortar with 5 % water solution of PAAm at 25 °C. Then the slurry was diluted by the excess of distilled water. The supernatant was decanted and the precipitant was washed several times by distilled water; after that it was collected and tested.

The total amount of PAAm, which adsorbed onto Fe MNPs was determined by TG/DSC thermal analysis. Fig. 5 presents

the thermograms for the initial Fe MNPs and MNPs encapsulated by PAAm.

Both pristine MNPs and encapsulated MNPs exhibit weight gain (Fig. 5A) in the process of heating. It is the result of the oxidation of iron by the atmospheric oxygen. There is clear difference in the total weight gain of these two samples. It stems from the decomposition of PAAm deposit on the surface of MNPs, which effectively decreases the weight gain. The difference of the weight gain is ca 14 %. This value corresponds to the PAAm deposit on the surface of MNPs. The thickness of this layer can be estimated using the residual amount of LPAAm on the surface of MNPs determined by thermal analysis. Corresponding conversion into volume fraction taking into account the difference in densities of PAAm and Fe core gives 40 % of polymer. The calculation of the thickness of a layer at the surface of the spherical particle with the diameter 90 nm gives ca 8 nm for the layer. Meanwhile, this value corresponds to the dry layer of polymer on the surface. If the MNPs are dispersed in water the polymeric layer swells and its thickness increases. If we assume that the conformation of PAAm macromolecules in the layer is a random Gaussian coil, the volume fraction of a polymer in a coil is given by the following relation:

$$\varphi_G = \frac{6^{3/2}}{8\sqrt{N}} \qquad (7)$$

N is the number of monomeric segments in the chain. The number of Kuhn segments for the molecular weight of PAAm (143.6 kDa) is N = 500, which in turn gives $\varphi_G = 0.08$. It is a reasonable estimation for the volume fraction of PAAm in a swollen Gaussian coil. Thus, in water the volume of PAAm layer increases by a factor of 1/0.08 = 12.5. Then, the thickness of a layer increases up to ca. 30 nm. (This value was used as a basic level in the theoretical calculations given above)

Fig. 6 presents multimodal distribution of particles/aggregates in water suspension of iron MNPs encapsulated by PAAm. PSD of iron MNPs in water suspension comprises two peaks. The first one is positioned at 160–200 nm. This peak most likely corresponds to individual Fe MNPs in suspension. The estimation of the characteristic dimensions of encapsulated particle, which comprises 84 nm Fe core and 30 nm PAAm steric protective layer on the surface gives ca 144 nm for the diameter. It is rather close to the position of the first peak at the PSD plot. The second mode is positioned at ca 1000 nm. This peal obviously stans for the aggregates of MNPs. The relative number fractions of these two peals are 90 % for the individual MNPs and 10 % for large aggregates. It means that individual MNPs dominate over aggregates in iron MNPs suspension. Qualitatively, this result is in agreement with the conclusions made based on the theoretical consideration, which favoured the possibility of de-aggregation of iron MNPs if sterically stabilized by protective layers.

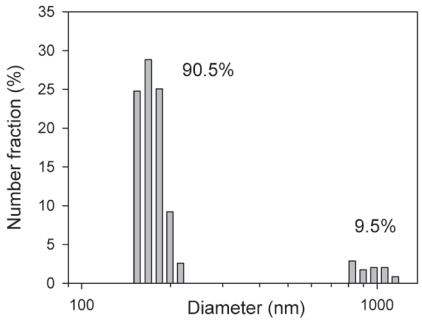

Fig. 6. Multimodal PSD of iron MNPs in water suspension by DLS

However, full de-aggregation was not achieved. The fraction of aggregates is still substantial. Most likely it is due to high polydispersity of MNPs. As it was shown in Theory section the energy of interaction among MNPs strongly depends on their radius. If the ensemble of MNPs is polydisperse, then there is a large fraction of particles with enhanced interaction. This fraction obviously provides aggregation which can not be prevented by 30 nm PAAm layers.

Conclusions

The factors of aggregation of Fe magnetic nanoparticles (mean diameter 84 nm) in water suspension were analyzed using extended DLVO (Derjaguin-Landau-Verwey-Overbeek) approach. It is based on the balance among Van der Waals, electrostatic, magnetic and steric interactions. It was shown that attractive magnetic and repulsive steric interactions dominate over other in suspensions of Fe MNPs. As a result of their superposing the dependence of the energy of interaction between MNPs exhibits minimum, which corresponds to the formation of aggregates of MNPs. If the depth of the minimum is less than 20 kT, the aggregates can be disrupted by the thermal motion. The depth of the minimum is very sensitive to the size of MNP, to its magnetization, and to the thickness of the layer on its surface. It was shown that for Fe MNPs 84 nm in diameter and magnetization 100 kA/m the threshold of the stability corresponds to the protective layer 30 nm. To test the theory Fe MNPs synthesized by electrical explosion of wire were encapsulated by polyacrylamide in water suspension to provide steric repulsion. It was shown that the fraction of PAAm in the protective layer is around 14 % and it resulted in the efficient diminishing of the aggregation of metallic iron MNPs in water.

Acknowledgement

Authors thank Dr. K. Balymov for performing the magnetic characterization of MNPs, Dr. A. I. Medvedev and Dr. A. M. Murzakayev for special support.

References

1. Huber DL. Synthesis, Properties, and Applications of Iron Nanoparticles. *Small.* 2005;1(5):482-501. DOI:10.1002/smll.200500006.
2. Llandro J, Palfreyman JJ, Ionescu A, Barnes CHW. Magnetic biosensor technologies for medical applications: a review. *Med Biol Eng Comput.* 2010;48(10):977–98. DOI:10.1007/s11517-010-0649-3.
3. Lu AH, Salabas EL, Schuth F. Magnetic nanoparticles: synthesis, protection, functionalization, and application. *Angew Chem Int Ed Engl.* 2007;46(8):1222–44. DOI:10.1002/anie.200602866.
4. Liu G, Gao J, Ai H, Chen X. Applications and Potential Toxicity of Magnetic Iron Oxide Nanoparticles. *Small.* 2013;9(9–10):1533–45. DOI:10.1002/smll.201201531
5. Hiemenz PC, Rajagopalan R. Principles of Colloid and Surface Chemistry. New York: Marcel Dekker, 1997. 499 p. ISBN9780824793975.

6. Kurlyandskaya GV, Bhagat SM, Safronov AP, Beketov IV, Larrañaga A. Spherical magnetic nanoparticles fabricated by electric explosion of wire. *AIP Adv.* 2011;1:042122. DOI:10.1063/1.3657510.
7. Beketov IV, Safronov AP, Medvedev AI, Alonso J, Kurlyandskaya GV, Bhagat SM. Iron oxide nanoparticles fabricated by electric explosion of wire: focus on magnetic nanofluids. *AIP Adv*. 2012;2:022154. DOI:10.1063/1.4730405.
8. Safronov AP, Kurlyandskaya GV, Chlenova AA, Kuznetsov MV, Bazhin DN, Beketov IV, Sanchez-Ilarduya MB, Martinez-Amesti A. Carbon Deposition from Aromatic Solvents onto Active Intact 3d Metal Surface at Ambient Conditions. *Langmuir*. 2014;30(11):3243–53. DOI:10.1021/la4049709.
9. Diguet G, Beaugnon E, Cavaillé JY. Shape Effect in the Magnetostriction of Ferromagnetic Composite. *J Magn Magn Mater*. 2010;322(21):3337–41. DOI:10.1016/j.jmmm.2010.06.020.
10. Sanchez-Dominguez M, Rodriguez-Abreu C. Nanocolloids: A Meeting Point for Scientists and Technologists. Netherlands: Elsevier, 2016. ISBN978-0-12-801578-0.
11. Walker DA, Kowalczyk B, de la Cruz MO, Grzybowski BA. Electrostatics at the nanoscale. *Nanoscale*. 2011;3(4):1316–44. Doi:10.1039/C0NR00698J.
12. Lim JK, Majetich SA, Tilton RD. Stabilization of Superparamagnetic Iron Oxide Core–Gold Shell Nanoparticles in High Ionic Strength Media. *Langmuir*. 2009;25(23):13384–93. DOI:10.1021/la9019734.
13. Rosensweig RE. Ferrohydrodynamics. USA: Dover books on physics, 2014. 344 p. ISBN9780486678344.
14. O'Handley RC. Modern Magnetic Materials. New York: John Wiley & Sons, 1972. 740 p. ISBN978-0471155669.
15. Jun YW, Seo JW, Cheon J. Nanoscaling Laws of Magnetic Nanoparticles and Their Applicabilities in Biomedical Sciences. *Acc Chem Res*. 2008;41(2):179–89. DOI:10.1021/ar700121f.

Cite this article as:
Shankar A, Safronov A, Beketov I. Encapsulation of metallic iron magnetic nanoparticles by polyacrylamide in water suspensions. *Chimica Techno Acta*. 2017;4(3):158–66. DOI:10.15826/chimtech/2017.4.3.01.